Resonant photoemission characterization of SnO

V. M. Jiménez, G. Lassaletta, A. Fernández, J. P. Espinós, F. Yubero, and A. R. González-Elipe*
Instituto de Ciencia de Materiales de Sevilla (CSIC, Universidad de Sevilla), and Departamento Química Inorgánica, Avenida Américo Vespucio s/n, 41092 Sevilla, Spain

L. Soriano and J. M. Sanz
Departamento Física Aplicada, Facultad de Ciencias C-XII, Universidad de Autónoma, Cantoblanco, 28049 Madrid, Spain

D. A. Papaconstantopoulos
Complex Systems Theory Branch, Naval Research Laboratory, Washington, D.C. 20375-5320
(Received 23 March 1998)

A thick layer of SnO, equivalent in its electronic properties to the bulk material, has been investigated by means of resonant photoemission and the mathematical method of factor analysis. This study has shown that O2p, Sn5s, and Sn5p partial density of states are the main contributions to the valence band of this material. The distribution through the valence band of these partial contributions has been determined by spectral subtraction and factor analysis of the resonance photoemission spectra, as well as by band structure calculation. The resonance behavior (i.e., change in intensity with the photon energy) of these three contributions has been analyzed. The Sn5p levels present a typical Fano-like behavior with a minimum intensity at about 28 eV and a maximum at 40 eV. The Sn5s partial density distribution also depicts a change in intensity as a function of the photon energy with a minimum situated at 35 eV and a maximum at 55 eV. Tentatively, this behavior has been linked to the existence of a broad absorption feature detected by electron energy loss spectroscopy and constant final state spectra, both depicting a broad maximum at about 50 eV. [S0163-1829(99)07339-7]

I. INTRODUCTION

Tin dioxide is a widely used material because of its applications as a gas sensor element or as transparent/conductive coating when doped with elements such as In, Cd, etc.[1–3] Due to this interest many characterization studies have been carried out on the electronic structure of tin oxides. Core level or valence band photoemission[4–8] have been widely used for the characterization of this material. One of the main issues of these studies is the analysis of the changes in stoichiometry that occur when SnO_2 is subjected to different reduction treatments including heating in CO or H_2 and Ar^+-sputtering.[4–5,9–10] Usually, formation of Sn^{2+} species is claimed as the main result of these treatments. Auger, x-ray photoemission spectroscopy (XPS), ultraviolet photoemission spectroscopy (UPS), electron energy loss spectroscopy (EELS), synchrotron photoemission, and resonant photoemission have been used to characterize the electronic state of these modified surfaces.[4–12] On the other hand, many of these studies have paid a particular attention to the electronic structure of stoichiometric SnO_2 and to this material partially reduced to a SnO_x ($x<2$) state, where it may be a mixture of different oxidation states of tin (i.e., Sn, Sn^{2+}, and Sn^{4+}). Different theoretical analyses of the occupied and empty states of tin oxide have also been carried out and their results compared with those of different experiments.[6,13,14]

Despite this interest in the electronic properties of SnO_2 and SnO_x ($1<x<2$), to our knowledge no experimental reports are available in the literature on the electronic structure of pure SnO. However, the study of the electronic properties of this material is interesting because it is the obvious reference compound to compare with SnO_x phases. Also, from a fundamental point of view, the electronic structure of SnO, typical of other post-transitional oxides such as SiO, PbO, GeO, etc., is interesting because of the involvement of occupied **n**s levels in the valence band of these materials.[13,14] This is the main reason for the big changes in the electronic properties of M^{II} and M^{IV} post/transition-metal oxides. Thus, while SnO_2 is a wide band-gap semiconductor (band gap 3.6 eV), SnO has electrical conductivity, a fact that has to be related with the filling of the Sn 5s levels by the so-called ''inert pair'' electrons.[13,14,15]

The present paper presents a synchrotron photoemission characterization of pure SnO. It reports a resonant photoemission study ($28\,\mathrm{eV}<h\nu<70\,\mathrm{eV}$) of the valence-band (VB) levels, together with some results by constant final state (CFS) spectroscopy and EELS to characterize the empty states of the system. To understand the origin of the different spectral features, our experimental results are compared with a theoretical calculation of the density of states of SnO, which provides a description of the valence band and partial density of states curves of this material. The mathematical method of factor analysis (FA) (Ref. 16) has been used for the analysis of the resonant photoemission spectra. This mathematical procedure is a general tool with other electron spectroscopies, where it is generally used to estimate the partition of single components in complex spectra.[17–19] Its use to analyze resonant photoemission spectra does not pretend to extract single component spectra, but to describe the distribution through the valence band of the partial electronic density of single state contributions and the change of their photoemission cross sections with the photon energy.

II. EXPERIMENT

The SnO was deposited on SiO_2 by evaporation from a SnO source consisting in a ceramic tube resistively heated. To avoid the formation of some traces of metallic tin, the deposits had to be exposed to O_2 under well-controlled conditions as reported in Ref. 20. Prior to the evaporation of SnO, the SiO_2 substrate, formed by a 200 Å-thick overlayer of SiO_2 grown on Si(111), was cleaned by mild bombardment with O_2^+ ions of 500 eV kinetic energy.

The photoemission experiments were performed in beamline TGM3 at the Berlin synchrotron radiation source (BESSY), equipped with a thoroidal grating monochromator and an ultrahigh vacuum station with a base pressure of 10^{-10} torr. Photoemission spectra, as a function of the deposited SnO, were measured using an ARES analyzer at constant pass energy of 25 eV and different photon energies between 28 and 70 eV. The angle of incidence of the *p*-polarized light was 45° with respect to the sample normal. All the spectra have been normalized to the photon flux as measured at a gold mirror at the entrance of the chamber.

The EELS spectra have been measured in our home laboratory in a VG-ESCALAB 210 spectrometer using a primary beam of electrons of 2000 eV kinetic energy.

III. BAND-STRUCTURE CALCULATION

We have performed self-consistent energy band calculations for SnO in the CsCl structure as a function of lattice parameter using the augmented plane wave (APW) method[21] in the local density approximation (LDA) of Hedin and Lundqvist.[22] Our LDA results give a total energy minimum at a lattice constant of 5.836 bohr. So we have used this lattice parameter to calculate the energy bands and the density of electronic states (DOS) by the tetrahedron method.[23] Our calculated DOS shows a very small gap at the Fermi level, which is characteristic of LDA calculations that typically underestimate the size of the energy gap in semiconductors and insulators. Otherwise our calculated DOS, within the assumption of crystalline CsCl structure, is reliable especially for the VB. The DOS and its angular momentum components are compared within our measurements in the discussion section.

IV. RESULTS

The VB spectra of SnO were investigated for a thick layer of SnO deposited for a long period of time, so that no contribution from the SiO_2 substrate could be detected in spectra recorded with $h\nu = 120$ eV to excite the Si2*p* levels. The formation of a pure phase of SnO under our experimental conditions was proved by the appearance of a single and well-defined doublet of the Sn4*d* level at a binding energy (BE) of 24.6 eV for the Sn4$d_{5/2}$ peak. The spectra, taken with different photon energies between 28 and 70 eV, are plotted in Fig. 1. It is apparent in these spectra that changes in the intensity of some of their features occur as a function of the photon energy. To follow in more detail these changes we have plotted in Fig. 2 (top) the height of the features with BE's of 2.0, 4.0, 5.8, and 8.6 eV as a function of the photon energy. In the sense of higher BE's they correspond, respectively, to the first and second maxima of the spectra, the subsequent shoulder and the last maximum of the spectra. The plots in Fig. 2 (top), which are equivalent to constant initial state (CIS) spectra,[24] show significant and different changes in the intensity for the four selected points. Thus, the CIS curve at 4.0, 5.8, and 8.6 eV present a minimum

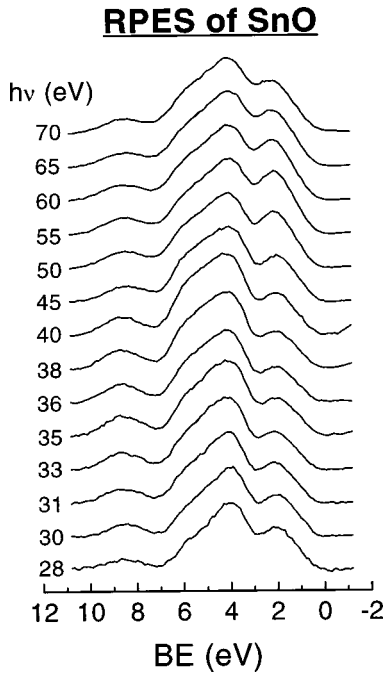

FIG. 1. Valence-band photoemission spectra for a thick layer of SnO recorded with different photon energies between 28 and 70 eV.

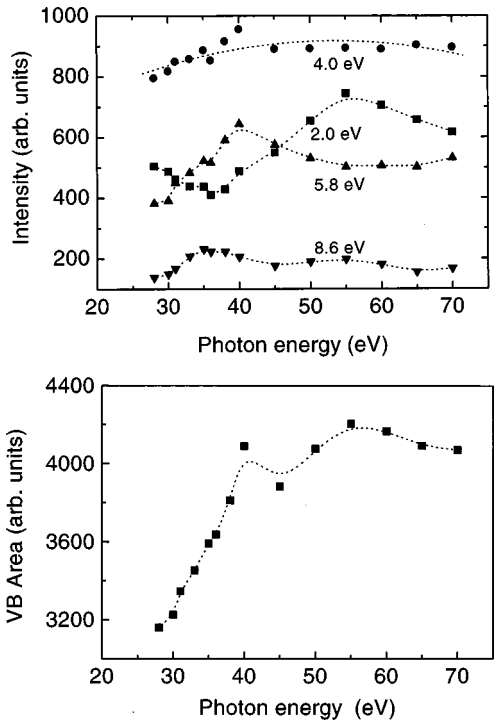

FIG. 2. Top: Evolution with the photon energy of the high of the spectral features at 2.0, 4.0, 5.8, and 8.6 eV taken from the valence-band spectra of Fig. 1. Bottom: Area of the valence band spectra in Fig. 1 as a function of the photon energy. Dotted lines are plotted to guide the eyes.

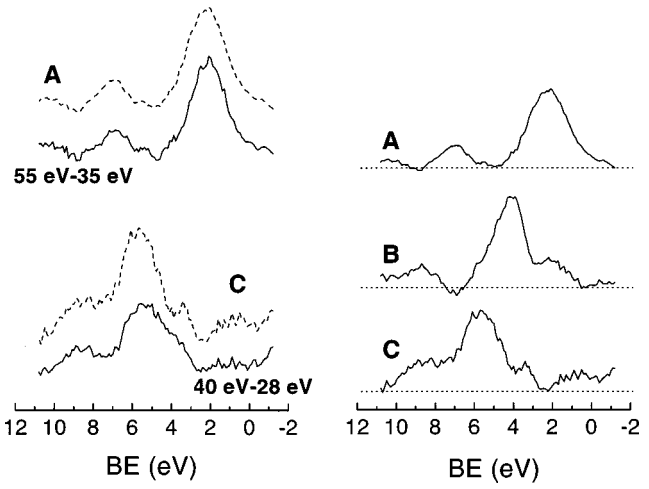

FIG. 3. Left: The difference spectra 55–35 eV and 40–28 eV (full line) and comparison with principal components *A* and *C* determined by FA (dashed lines). Right: Shape of the principal components determined by FA that reproduces the spectra in Fig. 1.

intensity at 28 eV [the minimum is not well defined in Fig. 2 (top) because photon energies below 28 were not available in our experiment]. Then, the intensity of the corresponding CIS spectra increases to reach a maximum at around 40 eV. The feature at 2.0 eV presents a different behavior, depicting a minimum at ~35 eV and a maximum at 55 eV. These changes in intensity correspond to some kind of resonance photoemission events, since equivalent changes in cross sections are not expected within this energy range.[25] A typical resonance process that has been discussed for SnO_2 corresponds to the enhancement of the Sn5*p* photoemission cross section through an additional $Sn4d \rightarrow Sn5p^*$ excitation channel (i.e., Fano-type resonance mechanism).[4]

Another clear indication of the existence of resonance phenomena affecting the VB spectra can be also seen in Fig. 2 (bottom) for the area of the whole valence-band spectra plotted against the photon energy. The curve shows significant changes in intensity with relative maxima at 40 and 55 eV, clearly reproducing the other changes affecting the single features of the spectra.

Besides these previous procedures, for the analysis of resonance photoemission spectra it is widely used the subtraction of an off-resonance spectrum from another at the maximum of the resonance process.[26–28] In this way, one obtains a difference spectrum which defines a zone of the valence-band spectra changing simultaneously in intensity with the photon energy. Since in a resonance process the enhancement in intensity is due to the increase of the cross section of a particular atomic orbital,[29] the difference spectrum can be taken as a description of the distribution through the valence band of hybridised states involving such atomic orbital (i.e., a description of the distribution of the partial density of states of that particular state). For the analysis of the VB spectra in Fig. 1, we have also applied this subtraction procedure. Figure 3 (left) shows as full lines the difference spectra 55-35 eV (i.e., the difference spectra obtained by subtracting the spectrum taken with 35 eV from that recorded with 55 eV) and 40-28 eV (i.e., difference spectrum obtained by subtracting the spectrum taken at 28 eV from that recorded at 40 eV). It is important to note that, according to Fig. 2, in the spectra taken with $h\nu = 55$ and 35 eV, the spectral feature at 5.8 eV has a very similar intensity, so that the spectral change is mainly due to the peak at 2.0 eV and other regions of the spectra with a similar variation in respect to the photon energy. The same can be said for the difference 40-28 eV, mainly reproducing the change affecting the feature at 5.8 eV and other associated zones of the spectrum. It is clear from Fig. 3 that the two difference spectra extend over a wide binding energy region and are not restricted to the maximum of the peaks taken to plot the CIS curves in Fig. 2.

Another procedure to obtain information about the distribution profile of the different contributions to the valence band is by using the FA methodology. Typically, FA is used for a quantitative assessment of the single components reproducing a series of spectra. Here, its use is intended as an alternative to the subtraction procedure described above. A detailed description of the method as applied to the spectra in Fig. 1 is presented in the Appendix. The main results of this analysis are that the full set of valence-band spectra are reproduced by three components whose shape is shown in Fig. 3 (right). The first one (*A*) presents maxima at 2.0 and 7.2 eV. The second (*B*) has a maximum at 4.0 and then different structures along the whole energy range of the VB spectrum. The third (*C*), with a maximum at 5.8 eV, has also a very well defined shoulder at 8.2 eV. Tentatively we associate these three curves with the distribution profiles of the Sn5*s*, O2*p*, and Sn5*p* partial contributions to the valence band. With this assignment, the peaks at 2.0, 4.0, and 5.8 eV would mainly have a Sn5*s*, O2*p*, and Sn5*p* character, respectively. Comparing the two panels of Fig. 3, it is apparent that components *A* and *C* depict a shape very similar to the difference spectra 55-35 eV and 40-28 eV, respectively. This good agreement supports that the results by FA are equivalent to those obtained by subtraction of spectra. In general, an advantage of FA is that it provides an automatic procedure to establish the number and shape of the independent components reproducing a set of spectra. In our case, this means that besides confirming the shape of the difference spectra 55-35 and 40-28, FA has permitted to determine the shape of a third contribution to the VB, tentatively attributed to the distribution profile of the O2*p* partial density of states (component *B*). In this respect, it is important to realize the physical meaning of the three components determined by FA. As for the difference spectra, these components are not an exact and quantitative representation of partial density of state curves, but a description of those regions of the experimental spectra whose intensity change simultaneously with the photon energy (i.e., due to changes in the photoemission cross section of a particular type of orbital). Since the resonant processes are atomic in nature they occur irrespective of the fact that the atomic levels are mixed to form a band with other atomic orbitals. Thus, the different spectra or the FA components can be taken as an approximate description of the distribution profile of partial density of state curves.

From an inspection of the shapes of components *A*-*C* in Fig. 3 (right), describing the distribution of Sn5*s*, O2*p*, and Sn5*p* states, it is clear that they extend over the whole energy region of the VB spectrum. It is also possible to conclude that the maximum at 8 eV has an important Sn5*p* contribution, the Sn5*s* levels contributing mainly to the spec-

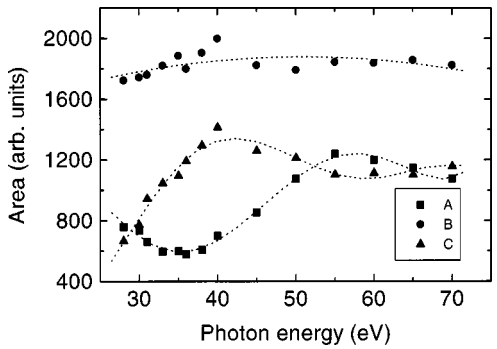

FIG. 4. Evolution with the photon energy of the intensity of the principal components *A* (Sn5*s*), *B* (O2*p*), and *C* (Sn5*p*) determined by FA. Dotted lines are plotted to guide the eyes.

tral region at around 7 eV. This conclusions is supported by the fact that the maximum at 8 eV of the experimental spectra shows an increase in intensity according to a similar behavior to that of the shoulder at 5.8 eV (see Fig. 2). However, such an assignment would be contradictory to previous valence band calculations of the electronic structure of SnO (6*c*, 6*d*, 13, 14) which account for a maximum around that photon energy as due to Sn5*s* derived states. We will come back to this point in the discussion.

Curves similar to those in Fig. 2 corresponding to the evolution of CIS intensities as a function of the photon energies, can be obtained by plotting the magnitude of components *A*, *B*, and *C* in each spectrum of the experimental series. Figure 4 shows the evolution of the magnitude of these three components determined by FA as a function of photon energies. We would like to stress that the curves in this figure represent the change in the photoemission cross section of each atomic level due to the resonant process. The shape of the plots of each component is very similar to that of the peaks at 2.0, 4.0, and 5.8 eV in the experimental spectra, a fact that supports that in the two cases we are figuring out the same type of change in the cross section due to resonant photoemission phenomena.

We have assumed that component *C* describes the distribution profile of Sn5*p* states through the VB. Therefore, it is reasonable to assume that the enhancement of its intensity when passing from $h\nu = 28$ to 40 eV is likely due to a Fano-type resonance process involving the Sn4*d* core-level states and where the dipole selection rule is preserved.[29] Component *B*, describing the distribution profile of O2*p* states through the VB also shows a slight enhancement of intensity around 40 eV. This small increase can be due to the fact that components *B* and *C* are not well separated by FA and that, therefore, some Sn5*p* contribution appears mixed with that of the O2*p* states. It has been tentatively assumed that component *A* describes the distribution profile of Sn5*s* levels. According to Figs. 2 and 3, this component depicts a minimum intensity at 35 eV and a maximum around 55 eV. This resonantlike behavior cannot be associated to the Sn4*d* core electron states in a Fano-type resonance; firstly because of the dipole selection rule controlling this type of transitions and secondly because the energy of the minimum is not compatible with the BE value of that core level. To find some clues that can explain the observed behavior, we have investigated the possible existence of other electronic transitions between occupied and unoccupied states in the energy range where it is observed the enhancement in the intensity of the *A* component. To map the empty states available for electronic transitions from occupied states, we have used EELS and CFS spectroscopies. EELS spectra, besides providing information about collective oscillation of electrons (i.e., plasma losses), furnish information about electronic transitions between occupied and unoccupied states. Experimental EELS raw data of SnO for a primary electron energy of 2000 eV have been reported previously.[20] In the present paper, the inelastic scattering cross section $K(\hbar\omega)$ has been obtained from the EELS raw data after subtraction of the multiple scattering background.[30] Optical properties as the dielectric function $\varepsilon(\hbar\omega)$ or the extinction coefficient $k(\hbar\omega)$ of the SnO thin film in the 5–80 eV energy range can be obtained by considering that the experimental cross section $K(\hbar\omega)$ is proportional to the electron loss function $\mathrm{Im}\{1/\varepsilon(\hbar\omega)\}$ and the use of the Kramers-Krönig relationship.[31] Figure 5 (left) shows a representation in a enlarged scale of the $k(\hbar\omega)$ function of SnO obtained from the EELS spectrum of SnO. For energies higher than 20 eV (i.e., close to the energy region measured by resonant photoemission) the $k(\hbar\omega)$ function depicts two features, a sharp one at ~28 eV, which has been attributed to transitions between the Sn4*d* levels and the conduction band,[32] and a very broad band extending in the energy region 40–60 eV and depicting a relative maximum at ~53 eV. The maximum of this latter band practi-

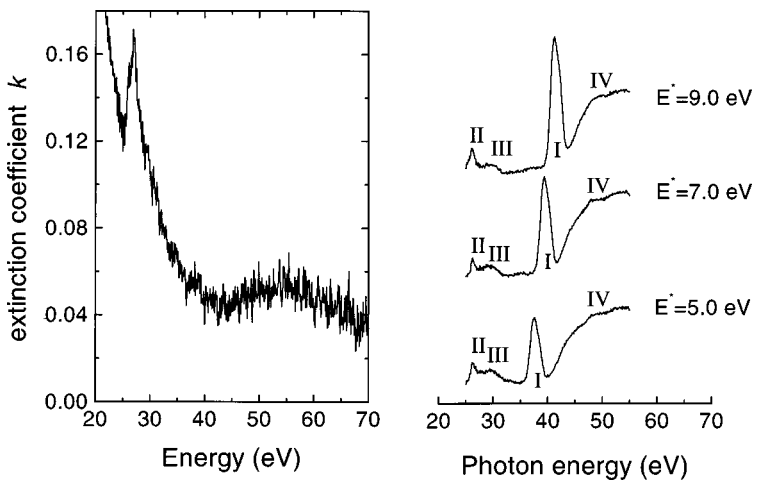

FIG. 5. Left: Extinction coefficient function *k* derived from EELS measurements of SnO. Right: CFS spectra of SnO for final kinetic energy of electrons of 5.0, 7.0, and 9.0 eV.

cally coincides with the resonant maximum of the resonant profile of the *A* component, a fact that supports that both phenomena might be connected. A structure appearing at a similar energy region can be also detected when looking at the CFS spectra of SnO. The spectra are collected by selecting electrons of a fixed kinetic energy with the electron analyser (i.e., partial electron yield detection), while the photon energy is swept through the desired energy range. These spectra furnish information about the empty states of the system by measuring the evolution of the absorption coefficient with the photon energy.[4] Figure 5 (right) also shows the CFS spectra of SnO as detected for photoelectrons at constant kinetic energies E^* of 5.0, 5.7, and 9.0 eV. Spectra for higher photoelectron energies were also recorded but they were shaded by the tail of secondary electrons and the contribution of higher harmonics of the radiation. In a series of CFS spectra of this kind, empty states correspond to peaks that appear always at the same value of the photon energy, whatever the kinetic energy of the recorded electrons.[4] In the CFS spectra of Fig. 5 (right) there are four well-defined structures, three of which always appear at the same photon energy. Structure I, which appears at different photon energies depending on the kinetic energy of the recorded electrons corresponds to the direct photoemission of the Sn4*d* levels. The two structures marked II and III, which stay fixed at 26.3 and 29.4 eV photon energies, can be attributed to excitons (pairs electron hole) formed by transitions from the filled Sn4*d* levels to the conduction band of the material. Similar structures have been observed by Themlin *et al.*[4] in CFS spectra of SnO_2 subjected to Ar^+ bombardment to induce its partial reduction. Taking into account that the Sn4*d* levels in SnO have a BE of ~25 eV, the structures II and III can be associated with empty states of the conduction band at approximately 1.1 and 4.2 eV above the Fermi level. It is likely that such states are involved in the resonance photoemission processes affecting the Sn5*p* contribution to the valence band. Also, they must be involved in the generation of the loss peak appearing at 28 eV, which we have attributed to an electronic transition from the Sn4*d* state (at 24.6 eV BE). Finally, structure IV, at an energy of ~47 eV, should correspond to some absorption process involving empty states at approximately that energy from an occupied state. The obtained value is in good agreement with the threshold energy of the broad band with a maximum at around 55 eV in the absorption coefficient curve deduced from the EELS spectra. This absorption feature could involve either the VB states or the Sn4*d* levels as occupied states. In any case, it is significant in relation to the resonance behavior of the VB spectra, that such an electronic transition occurs at an energy, which is within the same order of magnitude that the maximum of the resonant profile of the Sn5*s* contribution to the VB (cf. Figs. 2 and 4).

V. DISCUSSION

The analysis of the resonant photoemission spectra of SnO has provided a description of the electronic structure of this material. Besides, we have monitored some of the electronic transitions occurring between occupied and empty states. The following points have resulted critical for this investigation and will be the subject of a separate discussion:

Valence-band states

The valence band spectra are formed by the mixing of three different atomic contributions that we have tentatively attributed to the O2*p*, Sn5*s*, and Sn5*p* electronic states of oxygen and tin. The energy distribution profiles of these atomic components determined by subtraction of spectra and by FA is in relatively good agreement with the density of state distribution curves previously reported in the literature.[6,13,14] However, most of these previous calculations are based in a molecular-orbital approach with clusters of a limited number of tin and oxygen atoms. For a more straightforward comparison with our results, we have carried out band structure calculations by the augmented plane (APW) method.[21] We present the corresponding partial and total DOS curves in Fig. 6. For this calculation we have assumed an idealised CsCl structure for SnO. Since the thin film prepared here is likely amorphous and the actual structure of tin monoxide consists of a distorted CsCl structure,[13] we assume that an undistorted CsCl lattice is a good approximation to our system. The total DOS curve is characterized by four defined structures that we will call **A**-**D** by the similarity of the shape of this calculated curve and the photoelectron spectra in Fig. 1. These four structures are predominantly O2*p* states, which are hybridized with Sn-*p* and Sn-*s* states (see the different scales of the partial DOS curves, indicating the almost negligible contribution of t_{2g}-Sn, e_g-Sn, and 2*s*-O curves). Thus, the first structure **A** corresponds mainly to hybridisation with Sn5*s* states, structure **B** has also some Sn5*s* character, while structure **C** results from hybridization between O2*p* and Sn5*p* states. The last structure **D** has a significant Sn5*s* character. From the comparison of the partial and total density-of-state curves and the photoelectron spectra in Fig. 2, it is apparent the similarity in shape and maxima distribution in the two sets of curves. This supports the previous tentative attribution of the peak features in the experimental spectra to the main maxima of Sn5*s*, Sn5*p*, and O2*p* contributions. The most significant difference between the experimental VB spectra and this theoretical DOS curve refers to the positions of these structures, since in the calculated VB curve, structures **A**, **B**, and **C** appear at closer positions in respect to the Fermi level (i.e., 1.0, 2.5, and 4.3 eV) than the equivalent features in the experimental spectra. Meanwhile, the maximum **D**, at ~8.3 eV with respect to E_f in the calculations, has a similar BE than the equivalent structure in the experimental VB spectra.

A significant discrepancy between the experiment and the present calculations and those existing in the literature based on dusters models[6,13,14] concerns the assignment of feature **D**. The theoretical calculations attribute this peak to Sn5*s* derived states mixed with O2*p* orbitals. On the contrary, in Fig. 3 subtracted spectra and calculated FA components show that O2*p* and Sn5*p* states are mainly responsible for the experimental maximum at that position. This agrees with the empirical resonant behavior of this feature, similar to that of the shoulder at 5.8 eV, due mainly to mixed Sn5*p* states (cf. Fig. 2). Moreover, according to the difference spectra and FA calculations, the Sn5*s* mixed states present their maximum contribution just below the Fermi edge, with a second relative maximum at around 7 eV in a position where there are no well-defined structures in the theoretical spectra.

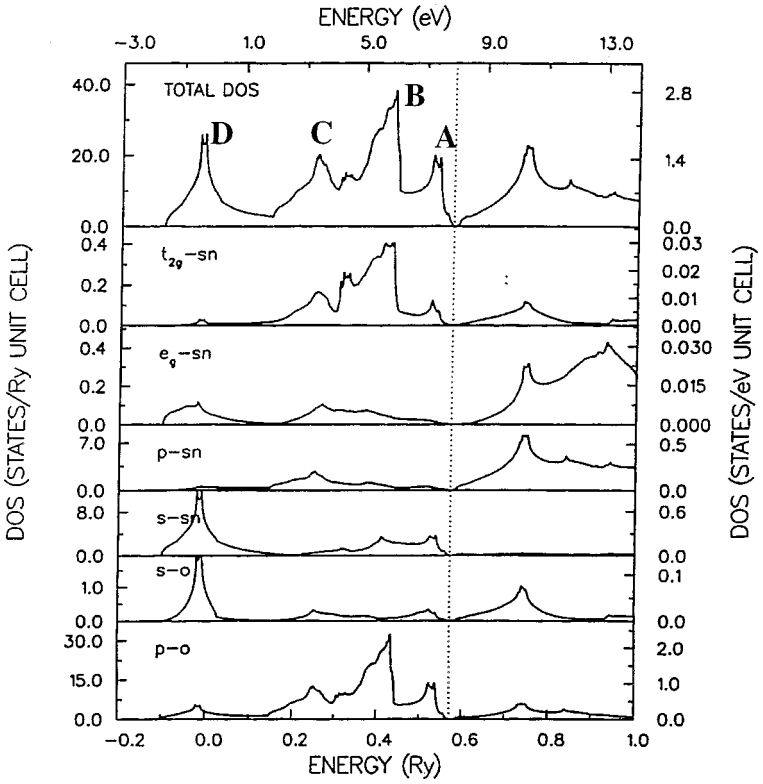

FIG. 6. Calculated DOS curves for SnO. The dotted line indicates the position of the Fermi level.

Within this picture, the resonant photoemission study clearly provides a clear experimental evidence about the distribution of electronic levels through the valence band. In this picture, it is critical that the Sn5*s* levels, hybridised with O2*p* states, constitute the highest occupied states of the system. Such contribution is recognized as the main factor for the differences in electronic properties between SnO and SnO_2.

Resonant photoemission and empty states

It has been shown that the Sn5*p* contribution to the valence band, depicting a main maximum at 5.8 eV and a second one at ~8–9 eV, changes in intensity with the photon energy. Its intensity profile can be associated with that of a Fano-like resonant mechanism. In fact, our analysis of the spectra has shown that the cross section of the Sn5*p* states changes with the photon energy. The shape of this change depicts a resonance profile characterized by a minimum at 28 eV and a maximum at 40 eV that can be explained by a Fano-type resonance mechanism.[29] This resonance implies an electronic process where, in a first step, the following electronic transition occurs:

$$4d^{10}(V)^n 5p^0(C) + h\nu \rightarrow [4d^9(V)^n 5p^1(C)]^*, \qquad (1)$$

where $5p^0(C)$ and $5p^1(C)$ are electronic states of the conduction band of the material. The existence of these states and the possibility of such electronic transitions has been shown by the EELS and CFS spectra presented in Fig. 5. Thus, the peak at 28 eV in the EELS spectrum must correspond to an electronic transition from the Sn4*d* levels (24.6 eV BE) to the empty states at 1.1 and/or 4.2 eV above the Fermi level. A similar mechanism has been invoked by Themlin *et al.*[4] in their analysis of the resonance photoemission behavior of defective SnO_2.

The excited electronic state referred in Eq. (1) may decay by the emission of an electron through an autoionization process:

$$[4d^9(V)^n 5p^1(C)]^* \rightarrow [4d^{10}(V)^{n-1} 5p^0(C)] + e^-. \qquad (2)$$

This process leads to the same final state as the direct photoemission from the VB, thus opening a second photoemission channel that leads to an increase in the photoemission cross section. Since in this type of resonance processes the dipole selection rule is always preserved,[29] an electronic transition involving Sn4*d* core levels will only produce an enhancement in the photoemission cross section of Sn5*p* partial density of states, as we had tentatively proposed in the previous section to explain the resonance behavior of component *C*. The existence of a large contribution to the conduction band of mixed Sn5*p* states is supported by the DOS curves in Fig. 6. A main maximum at approximately 2.5 eV above the Fermi level is the leading peak of the distribution of unoccupied states. These structures have mainly a Sn5*p* and O2*p* characters, with practically no contribution from Sn5*s* states. The peaks at 1.1 and 4.2 eV above the Fermi level observed in the CFS spectra in Fig. 5 (right) are produced by transitions from the Sn4*d* to Sn5*p* states, thus supporting the calculated DOS curves in Fig. 6.

The analysis of the VB spectra has shown that the Sn5*s* contribution, depicting a main maximum at 2 eV and a second one at 7–8 eV, changes in intensity with the photon energy. Its intensity profile presents a maximum at a photon energy at which there is an optical absorption process, as shown by EELS and CFS spectra. Since the Sn4*d* levels are

the only core level states of tin available in the energy range swept in our experiment, owing to the dipolar selection rules no resonance enhancement of photoemission intensity should be expected for the zones of the VB spectra with a significant Sn5*s* character. However, our analysis of the BV spectra has shown that the distribution profile of the Sn5*s* contribution to the valence band depicts a variation of its intensity, showing a minimum at 35 eV and a maximum at 55 eV. The origin of this enhancement of the Sn5*s* intensity is still unclear. A possibility could be that it is linked with the Sn5*p* resonance due to the hybridization between the Sn5*p* an Sn5*s* levels. In the already referred paper of Themlin *et al.*,[4] these authors have shown that the Sn5*s* states depict an enhancement in intensity associated to that of the Sn5*p* states. However, we rather believe that it corresponds to another independent process associated with the broad absorption feature revealed by CFS and EELS at ~50 eV (cf. Fig. 5). Although the initial and final states involved in this transition are not known, we can assume that its occurrence brings the system to an excited state. From this situation the system might decay by the emission of an electron in a similar way as for the Fano mechanism schematized in Eqs. (1) and (2), thus leading to the same final state than by direct photoemission from Sn5*s* derived states. In previous resonant photoemission studies of transition-metal oxides, it has been found that resonance enhancement of valence-band intensity may depict a complex profile where, after the well-characterized Fano enhancement, there may be a broad shape increase in intensity (i.e., similar to that observed in Fig. 2 bottom).[28,33,34] The physical origin of the second broad feature is the subject of some controversy and a possible line for its explanation could be connected with the existence of electronic transitions as those shown in Fig. 5 for SnO.

VI. CONCLUSIONS

The valence band structure of SnO has been studied by resonance photoemission by recording the spectra at different photon energies. The analysis of these spectra has provided a way to establish the distribution in energy of the O2*p*, Sn5*p*, and Sn5*s* contributions to the VB. It has also accounted for the origin of the changes in intensity that undergoes the different peaks of the spectra. The obtained results are in relatively good agreement with the partial DOS curves obtained by calculation of the valence-band structure of SnO. Maxima of the spectra appear at 2, 4, 5–6, and 8–9 eV. They have been correlated with the maxima of the partial density of states of the distribution of Sn5*s*, O2*p*, and Sn5*p* states.

Resonant enhancement in the intensity of some of the components of the spectra has been found as a function of the photon energy. The resonant profile of the Sn5*p* density of states follows a typical Fano behavior with a minimum at about 28 eV, close to the Sn4*d* BE, and a maximum at 40 eV. The Sn5*s* density of states also depicts an enhancement in its intensity as a function of the photon energy, but in a different energy range than for the Sn5*p* density of states. In this case the minimum appears at 35 eV and the maximum at 55 eV. The fact that an absorption process is detected at about the same energy permits to suggest that both phenomena, resonant photoemission and absorption, might be linked.

Determination of empty states has been carried out by EELS and CFS spectroscopies. Two differentiated states at 1.1 and 4.2 eV above the Fermi level are likely involved in the resonance photoemission of Sn5*p* states. Other empty states, proved by a broad electronic transition with a threshold energy of ~47 eV, are likely involved in the resonance enhancement of the photoemission cross section of Sn5*s* levels.

ACKNOWLEDGMENTS

We thank the CICYT (Project No. MAT97-689) and the DGICYT (Project No. PB96-0061) for financial support. The synchrotron measurements have been taken at BESSY thanks to a UE grant of the HCM program.

APPENDIX: FACTOR ANALYSIS OF VALENCE-BAND SPECTRA OF SnO

Factor analysis is a powerful mathematical procedure based on a matricial analysis of spectra that has been used to analyze data from different spectroscopies. Auger,[17] XPS,[18] and x-ray appearance near-edge structure (Ref. 19) spectra have been analyzed by this method which, in many cases, has permitted to find out the actual shape and concentration of the elemental components that reproduce an experimental spectrum. To our knowledge, the present paper represents the first essay of applying FA to a series of VB resonant photoemission spectra. It is important to recall that the way in which we intend to use this procedure here is to figure out the distribution through the valence band of particular level contributions. VB states are the result of the hybridization of these single levels to form a band and the changes that we observe in the band states are produced because of the dependence on photon energy of the cross sections of the atomic levels due to the resonance phenomena (cf. Fig. 4).

Details about the principles and procedure of FA can be found in several reviews and books.[16] Here, we consider convenient to say a few words about the practical use of this procedure and about their possibilities. A first step in the calculation procedure is the determination of the actual number of principal components (PC) that reproduce all the spectra of a experimental series. The second step is the determination of the shape and relative concentration of these principal components in each spectrum of the series. The FA carried out here took as basis for the calculations all the spectra shown in Fig. 1, corresponding to the valence-band photoemission spectra of SnO recorded with different photon energies between 28 and 70 eV after background subtraction. The determination of the number of PC's existing in this experimental series implies a matricial analysis consisting of rotation and diagonalization of a matrix formed by all the data points of these spectra (each spectrum defining a column vector of the matrix). The result of this analysis is shown in Table I reporting the eigenvalues of the diagonal matrix obtained by this calculation and a series of parameter functions. Two basic criteria are used to decide the number of principal components: the number of significant eigenvalues and the number of spectra for which the IND function (i.e., indicator) presents a minimum. In this case the two criteria points to that the experimental series in Fig. 1 can be

TABLE I. Determination of the number of significant components that by lineal combination reproduce the spectra in Fig. 1.

N^o spectrum	Eigenvalue	RE[a]	IE[b]	IND[c]
1	2.96×10^{8}	42.01	11.22	0.2486
2	2.22×10^{6}	19.52	7.37	0.1355
3	3.00×10^{5}	13.77	6.37	0.1139
4	8.25×10^{4}	11.85	6.33	0.1186
5	5.00×10^{4}	10.50	6.27	0.1296
6	4.23×10^{4}	8.96	5.86	0.1401
7	2.44×10^{4}	7.93	5.60	0.1619
8	2.02×10^{4}	6.75	5.10	0.1875
9	1.23×10^{4}	5.85	4.69	0.2340
10	6.06×10^{3}	5.50	4.65	0.3438
11	5.64×10^{3}	4.98	4.41	0.5535
12	4.55×10^{3}	4.29	3.97	1.0727
13	2.47×10^{3}	4.04	3.89	4.0461

[a]Error function.
[b]Imbedded error.
[c]Indicator function.

reproduced by the lineal combination of *three* independent PC's.

To determine the shape of these components we proceed according to the usual ''target transformation analysis'' by which ''test factors'' with a shape similar to the actual ''principal components'' are transformed into these ones.[16,18] To obtain these test factors we have carried out a fitting analysis of one spectrum of the series. The fitting requires four bands that we have named a-d. These bands have been used as test factors for the target transformation analysis. Since there are only three components, we have considered that the sum of two of these bands is a suitable test factor for this analysis, the other two being the remaining two bands. Thus, we have considered two different sets of test factors. A first one consists of bands $a+d$, b and c and a second one a, b, $c+d$. The results of the target transformation analysis for these two sets is shown in Fig. 4. Surprisingly, the two sets furnish very similar shape for the PC's, thus supporting the validity of the final result. Moreover, the analysis gives the partition of each component in each experimental spectrum. By multiplying these partition values by the area of each PC's one obtains the intensities of Fig. 5 showing the resonance behavior of these three components.

A poorer agreement in the reproduction of the experimental spectra is obtained by considering only two PC's. In this case, one of the components has a shape similar to that of component A, while the second approaches the sum of components $B+C$ (cf. Fig. 3, right). The evolution of the intensities of these two components with the photon energy resembles in shape that of components A and B in Fig. 4. However, the option of three independent components, besides yielding a better reproduction of the experimental spectra, has a stronger physical basis because the VB of SnO is the result of the hybridisation of three different electronic levels (i.e., O2p, Sn5s, and Sn5p) whose resonant behavior with the photon energy should be different.

*Author to whom correspondence should be addressed. FAX: 34-05-4460665. Electronic address: Agustin@cica.es

[1] L. Davis, Thin Solid Films **236**, 1 (1993).
[2] A. L. Dawar, A. Kumar, S. Sharma, K. N. Tripathi, and P. C. Mathur, J. Mater. Sci. **28**, 639 (1993).
[3] W. Göpel and K. D. Schierbaum, Sens. Actuators B **26/27**, 1 (1995).
[4] J. M. Themlin, R. Sporken, J. Darville, R. Candano, J. M. Gilles, and R. L. Johnson, Phys. Rev. B **42**, 11 914 (1990).
[5] J. M. Themlin, M. Chtaïb, L. Henrard, P. Lambin, J. Darville, and J. M. Gilles, Phys. Rev. B **46**, 2460 (1992).
[6] R. Sanjinés, C. Coluzza, D. Rosenfeld, F. Gozzo, Ph. Almerás, F. Lévy, and G. Margaritondo, J. Appl. Phys. **73**, 3997 (1993); R. Sanjinés, D. Rosenfeld, F. Gozzo, Ph. Almerás, L. Pérez, F. Lévy, G. Margaritondo, and W. H. Schreiner, Surf. Interface Anal. **22**, 372 (1994); L. Köver, G. Moretti, Zs. Kovács, R. Sanjinés, I. Cserny, G. Margaritondo, J. Pálinkás, and H. Adachi, J. Vac. Sci. Technol. A **13**, 1382 (1995); L. Köver, Zs. Kovács, R. Sanjinés, G. Moretti, I. Cserny, G. Margaritondo, J. Pálinkás, and H. Adachi, Surf. Interface Anal. **23**, 461 (1995).
[7] J. M. Themlin, J.-M. Gilles, and R. L. Johnson, J. Phys. IV **4**, 183 (1994).
[8] P. de Padova, M. Fanfoni, R. Larciprete, M. Mangiantini, S. Priori, and P. Perfetti, Surf. Sci. **313**, 379 (1994).
[9] C. S. Fang, F. M. Pan, W. S. Tse, and S. R. Horng, Surf. Sci. **211/212**, 279 (1989).
[10] D. F. Cox, T. B. Fryberger, and S. Semancik, Phys. Rev. B **38**, 2072 (1988).
[11] D. F. Cox and G. B. Hoflund, Surf. Sci. **151**, 202 (1985).
[12] G. B. Hoflund and G. R. Corallo, Phys. Rev. B **46**, 7110 (1992).
[13] J. Terra and D. Guenzburger, Phys. Rev. B **44**, 8584 (1991).
[14] M. J. Terpstra, R. A. de Groot, and C. Haas, Phys. Rev. B **52**, 11 690 (1995).
[15] Z. M. Jarzabski and J. P. Marton, J. Electrochem. Soc. **123**, 199c (1976).
[16] E. R. Malinowski and D. G. Howery, *Factor Analysis in Chemistry* (Wiley, New York, 1980).
[17] S. Hofmann and J. Steffen, Surf. Interface Anal. **14**, 59 (1989).
[18] A. R. González-Elipe, J. P. Holgado, R. Alvarez, and G. Munuera, J. Phys. Chem. **96**, 3080 (1992).
[19] V. M. Jiménez, A. Caballero, A. Fernández, J. C. Sánchez-López, A. R. González-Elipe, J. F. Trigo, and J. M. Sanz, Surf. Interface Anal. **25**, 707 (1997).
[20] V. M. Jiménez, A. Fernández, J. P. Espinós, and A. R. González-Elipe, Surf. Sci. **350**, 113 (1996); V. M. Jiménez, J. A. Mejías, J. P. Espinós, and A. R. González-Elipe, *ibid.* **366**, 545 (1996); V. M. Jiménez, J. P. Espinós, and A. R. González-Elipe, *ibid.* **366**, 556 (1996).
[21] L. F. Mattheiss, J. H. Wood, and A. C. Switendick, *Methods in Computational Physics* (Academic, New York, 1968), Vol. 8.
[22] L. Hedin and B. I. Lundqvist, J. Phys. C **4**, 2064 (1971).
[23] G. Lehmann and M. Taut, Phys. Status Solidi **54**, 469 (1972).
[24] R. Patel, H. Höchst, G. W. Zajac, Sh. Pei, and J. Faber, J. Electron Spectrosc. Relat. Phenom. **68**, 461 (1994).
[25] J. J. Yeh and I. Lindau, At. Data Nucl. Data Tables **32**, 1 (1985).

[26] V. E. Henrich, Surf. Sci. **284**, 200 (1993).
[27] J. Nerlov, Q. Ge, and P. J. Moller, Surf. Sci. **348**, 28 (1996).
[28] C. Morant, A. Fernández, A. R. González-Elipe, L. Soriano, A. Stampfl, A. M. Bradshaw, and J. M. Sanz, Phys. Rev. B **52**, 11 711 (1995).
[29] L. C. Davis, J. Appl. Phys. **59**, R25 (1986).
[30] S. Tougaard and I. Charkendorff, Phys. Rev. B **35**, 6570 (1987).
[31] F. Yubero and S. Tougaard, Surf. Interface Anal. **19**, 269 (1992).
[32] A. J. Bevolo, J. D. Verhoeven, and M. Noack, Surf. Sci. **134**, 499 (1983).
[33] Z. Zhang, S.-P. Jeng, and V. E. Henrich, Phys. Rev. B **43**, 12 004 (1991).
[34] J. R. Lince, S. V. Didziulis, and J. A. Yarmoff, Phys. Rev. B **43**, 4641 (1991).